Strong electron correlation effects in nonvolatile electronic memory devices

M. J. Rozenberg[a)]
Laboratoire de Physique des Solides, UMR8502 Université Paris-Sud, Orsay 91405, France, and Departamento de Física Juan José Giambiagi, FCEN, Universidad de Buenos Aires, Ciudad Universitaria Pabellón I, (1428) Buenos Aires, Argentina

I. H. Inoue
Correlated Electron Research Center (CERC), National Institute of Advanced Industrial Science and Technology (AIST), Tsukuba 305-8562, Japan

M. J. Sánchez
Centro Atómico Bariloche, (8400) San Carlos de Bariloche, Argentina

(Received 14 June 2005; accepted 13 December 2005; published online 19 January 2006)

We investigate hysteresis effects in a model for nonvolatile memory devices. Two mechanisms are found to produce hysteresis effects qualitatively similar to those often experimentally observed in heterostructures of transition metal oxides. One of them is a switching effect based on a metal-insulator transition due to strong electron correlations at the dielectric/metal interface. The observed resistance switching phenomenon could be the experimental realization of a strongly correlated electron device. © *2006 American Institute of Physics*. [DOI: 10.1063/1.2164917]

The inclusion of strong correlation effects in semiconductor electronic devices has long been a goal of solid-state physicists. Significant progress has been achieved in recent years in studies of metal-insulator-metal (MIM) structures that display different types of resistance switching by the application of a voltage or current pulse; a prototype of two-terminal nonvolatile random access memories. The insulator of the MIM structure is either a transition metal oxide[1–6] or an organic material,[7,8] in which the electron correlations usually play an important role. The switching is directly related to the large hysteresis observed in the *I-V* characteristics.

The goal of the present work is to investigate the qualitatively different hystereses of *I-V* curves in the MIM structures that have been experimentally observed so far, and to associate each hysteresis type to an appropriate physical mechanism. Our starting point is a recently introduced model for the MIM device.[9] The model assumes the existence of an insulating (and inert) medium with a nonpercolative structure of metallic domains that might correspond to defects, nanoscale grains, phase-separated regions.[10] Smaller domains are closer to the electrodes and are called "top" and "bottom." A large domain occupies the bulk of the system that is called "central." Carriers tunnel between domains under the action of an external electric field (or applied voltage). The probability of charge transfer depends on phenomenological parameters such as the tunneling rates, the number of states in the domains, and their occupation (see Ref. 9 for details). As current is carried along various local paths, it scales with the area of the electrodes/dielectric interface. For simplicity, here we shall ignore disorder effects and take the total number of states of all "top" and "bottom" domains to be identical; i.e., $N_t = N_b$. We also take a unique tunneling rate for the two interfaces Γ^{ext} and similarly inside the dielectric Γ^{int}. Therefore, we can just consider the behavior of the "average" top and bottom domain occupations, which we denote n^t and n^b, respectively. The metallic electrodes are assumed half-filled.

The model of Ref. 9 is thus defined by a set of three coupled nonlinear differential equations,

$$\frac{dn^b}{dt} = \left[\Gamma^{\text{ext}} \frac{N_e}{2}(1 - n^b) - \Gamma^{\text{int}} n^b N_c (1 - n^c) \right] f(V), \tag{1}$$

$$\frac{dn^c}{dt} = [\Gamma^{\text{int}} N_b n^b (1 - n^c) - \Gamma^{\text{int}} n^c N_t (1 - n^t)] f(V), \tag{2}$$

$$\frac{dn^t}{dt} = \left[\Gamma^{\text{int}} N_c n^c (1 - n^t) - \Gamma^{\text{ext}} n^t \frac{N_e}{2} \right] f(V), \tag{3}$$

which have to be solved for the unknown $n^\alpha(t)$ with $\alpha = t, c, b$. The coefficients $f(V)$ are time dependent through the applied voltage protocol $V(t)$ and are assumed to be independent of α. There is no general solution for this model, so that we numerically solve for the system of diferential equations.

Let us now turn to the predictions of the model for the *I-V* characteristics and hysteresis effects. The applied voltage protocol is $0 \to V_{\max} \to -V_{\max} \to 0$ with a constant sweep velocity. For simplicity, all three domains are assumed to be initially half-filled. Following Simmons and Verderber,[11] we take the function $f(V) = \sinh(kV)$, where k depends on various material parameters; thus, we set $k = 1/\text{V}$. The (positive) current in and out of the system is given by the carriers entering the bottom domain and leaving the top domain respectively, thus their units are carrier per unit of time. In Fig. 1, we show the results for two qualitatively different hystereses that the model predicts depending on the choice of parameters. The current out (for current in, a similar analysis can be done) depends mainly on the filling level of the top domains. The larger their occupation, the more carriers that are available to tunnel out. During the positive side of the voltage protocol, V is initially increased and then decreased down to zero. During this phase, charge is transferred from the center domain to the top and from there to the electrode. Therefore, if more charge enters the top domain than leaves it, the filling level during the increasing positive-V ramp

[a)]Electronic mail: rozenberg@lps.u-psud.fr

 © 2006 American Institute of Physics
Downloaded 16 Feb 2006 to 200.0.233.52. Redistribution subject to AIP license or copyright, see http://apl.aip.org/apl/copyright.jsp

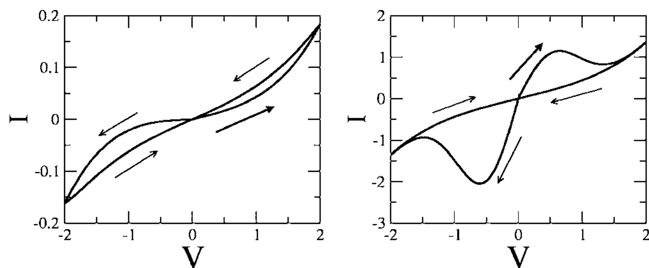

FIG. 1. Current-voltage *I-V* characteristics. $N_t = N_b = 10^6$, $N_c = 10^{10}$, $\Gamma^{\text{int}} = 2 \times 10^{-8}$, and $\Gamma^{\text{ext}} = 6 \times 10^{-14}$ (left panel) or $\Gamma^{\text{int}} = 8 \times 10^{-9}$, $\Gamma^{\text{ext}} = 6 \times 10^{-12}$ (right panel). The *V* protocol cycle begins at the thick arrow. The current *I* is in units of number of carriers per unit of time, and the voltage *V* is in units of volts $(k = 1/\text{V})$.

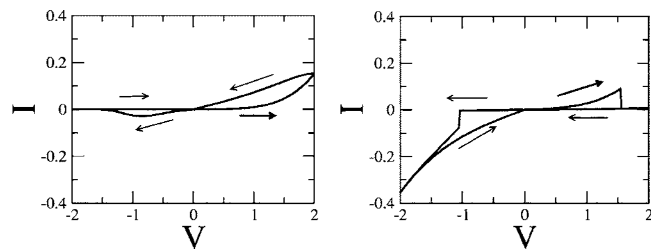

FIG. 2. Current-voltage characteristics. $N_t = N_b = 10^6$, $N_c = 10^{10}$, $\Gamma^{\text{int}} = 6 \times 10^{-8}$, $\Gamma^{\text{ext}} = 10^{-13}$, and $n^t(0) = n^b(0) = n^c(0) = 0.1$. Basic model with interface charge-dependent tunneling (top left), with occupation-driven Mott transition, and $\Delta/T = 3$ (top right). The *V* protocol cycle begins at the thick arrow. The current *I* is in units of number of carriers per unit of time, and the voltage *V* is in units of volts $(k = 1/\text{V})$.

would be lower than the filling level during the subsequent decreasing positive-*V* ramp. This would lead to low-to-high current switching, as shown in the left panel. Therefore, the qualitative form of the hysteresis depends on the intrasystem (top/center and bottom/center) charge transfers compared to the interface (top/electrode and bottom/electrode) ones, both of which are controlled by the model parameters (basically the ΓN products). Assuming a larger *interface*, transfers should be appropriate for systems such as Au/SiO/Au studied in the pioneering work of Simmons *et al.*[11] where hysteresis and negative differential resistance were observed and qualitative agreement with our model is found, as shown in the right panel of Fig. 1. On the other hand, larger *intrasystem* transfer is a likely assumption for the heterostructures with transition metal oxide dielectric, where electronic inhomogeneous states are often realized. It would also be the case for the system of artificially created domains of Al nanoclusters, where, in fact, hysteresis similar to the results shown in the left panel of Fig. 1, has been observed.[7]

While the present model provides useful insight for the analysis of relaxation times and basic switching mechanisms,[9] the qualitative predictions for hysteresis effect illustrated above show a notable limitation; namely, the *I-V* curves *never cross* at the origin. Experimentally, *crossing* *I-V* characteristics are often observed,[1,3,4,8] thus providing an important motivation to consider two extensions of the basic model [Eqs. (1)–(3)], which we shall describe next.

The first one is to incorporate the physics of interface tunneling rates that depend on the charge accumulation; that is, the dependence of Γ^{ext} with n^t and n^b. The underlying physical mechanism is similar to the dependence of the depletion width with impurity concentration in ohmic contacts of metal/semiconductor interfaces.[12] Basically, the accumulated charge density at the interface produces additional band bending that leads to a reduction in the tunneling barrier, thus enhancing Γ^{ext}. Borrowing from standard junction tunneling theory[12] we can qualitatively model this dependence as $\Gamma^{\text{ext}}_{t,b} = e^{-1/\sqrt{n^{t,b}}+1}\Gamma^{\text{ext}}$ (Ref. 13) so that, the tunneling is enhanced with increasing charge accumulation in the small interface domains right up to the saturation value Γ^{ext} for fully occupied domains; that is, $n^{t,b} = 1$. This mechanism is widely assumed to be relevant for many resistance switching phenomena; however, it is also usually linked to *poor nonvolatility* characteristics. We incorporated this effect in our basic set of Eqs. (1)–(3) by replacing the tunneling parameters Γ^{ext} with the occupation-dependent tunneling expressions described in the previous paragraph, and solved for the model behavior. The results are shown in Fig. 2 (left). We see that, in fact, this additional assumption is sufficient to turn the hysteresis into the *crossing* type, a result that can be understood through an analysis similar to that we described earlier. An important point to mention here is that the hysteresis effect does not necessarily need to take place at both electrodes simultaneously, since the large center domain acts as a buffer that effectively decouples the two interfaces. Hence, this mechanism would also be relevant for systems with two different interfaces where the switching properties are controlled by one of them. For example, in heterostructures such as $\text{Au/SrRuO}_3\text{/SrTi}_{0.99}\text{Nb}_{0.01}\text{O}_3$, where the $\text{SrRuO}_3\text{/SrTi}_{0.99}\text{Nb}_{0.01}\text{O}_3$ interface forms a Schottky barrier but Au/SrRuO_3 does not.[14]

As we mentioned before, the interphase charge accumulation mechanism is often linked with poor nonvolatile characteristics, possibly because it lacks a stabilization effect that could lengthen the lifetimes of the charge-accumulated (or -depleted) metastable states. A physical effect that would enable such stabilization is likely to be due to a *coherent* effect in which many particles act in a correlated manner. Here we propose that such a mechanism is based on a Mott metal-insulator transition taking place in the domains when they become close to half-filling.[3,15] In fact, this occupation- (or doping-) driven metal-insulator transition is a strong correlation effect found throughout the transition metal oxide series[16] and even in some organic materials.[17] For concreteness, we shall assume that the domains undergo a Mott transition when they are close to half-filling. On becoming insulating, the domains open an insulating gap Δ in their excitation spectrum, which we model by assuming a reduction in the density of states at the Fermi energy given by $D = e^{-\Delta/T}D_0$, T being the temperature. The dependence of the density of states at the Fermi energy was entered implicitly in our equations through a multiplicative factor (set to unity) in the function $f(V)$, since we were always concerned with tunneling between metallic domains. We now consider this effect explicitly by modifying $f(V)$ in the model Eqs. (1)–(3) to $f_{\text{mit}}(V) = e^{-\Delta/T}f(V)$ if the occupation of the corresponding domain is within 10% of half-filling, or else $f_{\text{mit}}(V) = f(V)$. The results are shown in Fig. 2 (right). The results can be understood as follows. Initially, the domains are assumed to be lightly filled; that is, in the metallic state. As the applied voltage is increased, charge is accumulated at the top domains, thus increasing their occupation level. Eventually, when they approach half-filling, they become insulating and open a Mott gap. The tunneling probability to and from the top domain gets dramatically reduced, with consequent drops in the output current and in the rate of further charge injec-

Downloaded 16 Feb 2006 to 200.0.233.52. Redistribution subject to AIP license or copyright, see http://apl.aip.org/apl/copyright.jsp

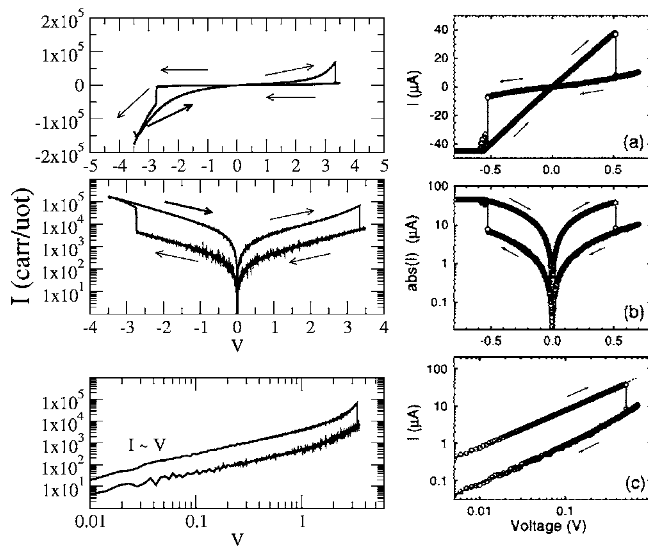

FIG. 3. *I-V* characteristics for the model with occupation-driven Mott transition. The model parameters are $N_t = N_b = 10^6$, $N_c = 10^9$, $\Gamma^{int} = 10^{-13}$, $\Gamma^{ext} = 3 \times 10$. The current I is in carriers per unit of time (Monte Carlo time step). The voltage protocol is $-V_{max} \rightarrow V_{max} \rightarrow -V_{max}$, similar as in the experiment. The voltage V is in units of volts ($k = 1/V$). in normal scale (top), semi-log scale (middle), and log-log scale (bottom). The right panels show experiments in $Au/SrZrO_3/SrRuO_3$ from Ref. 1.

tion. With the reduced charge injection, the occupation level of the domain remains about constant and the current is low for the rest of the positive voltage sweep ($\rightarrow V_{max} \rightarrow 0$). This is also the case for the beginning of the negative voltage sweep, as the *leakage* of charge out of the top domain is also greatly suppressed (*thus providing an enhanced nonvolatility of the high resistance state*). Eventually, a large negative V drives enough charge out of the top domains and once again they become metallic, their correlation gap closes, and the system switches back to a high current state.

In order to give further support to this mechanism we performed Monte Carlo simulations[9] on the model given by Eqs. (1)–(3) supplemented with the Mott transition effect. We looked for parameters that qualitatively reproduce the experimental results in the MIM structures with Cr-doped $SrTiO_3$ or $SrZrO_3$ of the IBM group.[1] Our results are shown in Fig. 3 and the experiments are shown in the inset. Not only is the qualitative agreement very satisfactory, several details are also worth pointing out. The initial occupation level of the domains that allow best comparison to the experimental data was found to be small (around 10%), consistent with the fact that the systems are nominally empty band insulators with only light doping due to the Cr substitution. Moreover, the intriguing sudden high-to-low current switching at positive applied bias in the experiment is a feature that naturally emerges from our domain-doping-driven metal-to-insulator transition scenario.

One final important point is that for all the various model variations that were discussed here, we have check that the basic resistance memory switching behavior under a pulsed voltage protocol is always observed. The results are always qualitatively very similar to those of Ref. 9 for the basic model. A systematic study of switching will be presented elsewhere.

To conclude, we have proposed a model for resistance memory switching and find the different physical mechanisms that lead to various qualitatively different hysteresis effects in the *I-V* characteristics. We proposed a scenario for memory switching in strongly correlated transition metal oxide heterostructures, based on a metal-insulator transition driven by charge injection (doping) to domain structures in physical proximity to interfaces. The information (high resistance state) is stored by driving the systems to a qualitatively different state which, at the same time, provides a mechanism for the enhancement of the nonvolatility. Our model results are supported by excellent qualitative agreement with experimental data in various heterostructures.

The authors would like to thank Y. Tokura, M. Kawasaki, A. Sawa, and A. Odagawa for valuable comments and discussions. We also acknowledge N. E. Hussey for critical reading of this paper. Support from Fundación Antorchas, UBACyT, Conicet, and ANCTyP is acknowledged.

[1] A. Beck, J. G. Bednorz, Ch. Gerber, C. Rossel, and D. Widmer, Appl. Phys. Lett. **77**, 139 (2000).
[2] S. Q. Liu, N. J. Wu, and A. Ignatiev, Appl. Phys. Lett. **76**, 2749 (2000).
[3] R. Fors, S. I. Khartsev, and A. M. Grishin, Phys. Rev. B **71**, 045305 (2005).
[4] A. Odagawa, H. Sato, I. H. Inoue, H. Akoh, M. Kawasaki, Y. Tokura, T. Kanno, and H. Adachi, Phys. Rev. B **70**, 224403 (2004).
[5] S. Seo, M. J. Lee, D. H. Seo, E. J. Jeoung, D.-S. Suh, Y. S. Joung, I. K. Yoo, I. R. Hwang, S. H. Kim, I. S. Byun, J.-S. Kim, J. S. Choi, and B. H. Park, Appl. Phys. Lett. **85**, 5655 (2004).
[6] E. Dagotto, Science **309**, 257 (2005).
[7] L. Ma, S. Pyo, J. Ouyang, Q. Xu, and Y. Yang, Appl. Phys. Lett. **82**, 1419 (2003).
[8] B. Mukherjee and A. J. Pal, Chem. Phys. Lett. **401**, 410 (2005); **85**, 2116 (2004).
[9] M. J. Rozenberg, I. H. Inoue, and M. J. Sánchez, Phys. Rev. Lett. **92**, 178302 (2004).
[10] K. Szot, W. Speier, R. Carius, U. Zastrow, and W. Beyer, Phys. Rev. Lett. **88**, 075508 (2002).
[11] J. G. Simmons and R. R. Verderber, Proc. R. Soc. London, Ser. A **301**, 77 (1967).
[12] S. M. Sze, *Physics of Semiconductor Devices* (Wiley, New York, 1981).
[13] H. C. Casey, *Devices for Integrated Circuits* (Wiley, New York, 1999).
[14] T. Fujii, M. Kawasaki, A. Sawa, H. Akoh, Y. Kawazoe, and Y. Tokura, Appl. Phys. Lett. **86**, 012107 (2005).
[15] C. A. Marianetti, G. Kotliar, and G. Ceder, Nat. Mater. **3**, 627 (2004).
[16] M. Imada, A. Fujimori, and Y. Tokura, Rev. Mod. Phys. **70**, 1039 (1998).
[17] H. Mori, M. Kamiya, M. Haemori, H. Suzuki, S. Tanaka, Y. Nishio, K. Kajita, and H. Moriyama, J. Am. Chem. Soc. **124**, 1251 (2002).

Downloaded 16 Feb 2006 to 200.0.233.52. Redistribution subject to AIP license or copyright, see http://apl.aip.org/apl/copyright.jsp